

Analysis of spatial arrangement of particles in thin foil of Al-Al₄C₃ material

M. BESTERCI, I. KOHÚTEK, K. SÜLLEIOVÁ

Institute of Materials Research, Slovak Academy of Sciences, Watsonova 47, 043 53 Košice, Slovak Republic

E-mail: kohutek@imrnov.saske.sk

I. SAXL

Mathematical Institute, Academy of Sciences of the Czech Republic, Žitná 25, 115 67 Praha 1, Czech Republic

TEM images of thin foils with quasi-globular particles are examined by means of two methods of spatial statistics. The spatial arrangement of particle reference points is described by means of *quadrat count* statistics and by *polygonal method* (the analysis of the Voronoi mosaic generated by patterns of particle reference points). A good agreement between the both approaches is found, the polygonal method is more sensitive and its results are more conclusive. © 1999 Kluwer Academic Publishers

1. Introduction

The properties of composite materials are influenced not only by the amount (volume fraction V_V) and dispersion (intensity λ – number of particles per unit volume) of strengthening phase, but also by its spatial organization (arrangement). This arrangement is at best revealed by considering the point pattern of particle reference points determined according to a convenient rule. Its description is model-based, which means that suitably chosen characteristics of given sample are evaluated and compared with characteristics of basic stochastic models of spatial arrangement [2, 7, 8, 11, 12]. Even when the statistical methods are well elaborated and successful in other areas, their usage in metallography is rather exceptional. In the present paper, thin foils of chosen composite material are analysed in order to answer three questions:

1. Is the dispersion of strengthening phase homogeneous w.r.t. the chosen sample size?
2. Is the arrangement of particle reference points in space uniform random (i.e., can the point patterns be considered as samples from a stationary Poisson point process)?
3. Are the features of clustering and/or hard cores present in the analysed point patterns?

The basic idea applied in the analysis is that the orthogonal projection of a parallel section sampled from a spatial stationary Poisson point process is a planar Poisson point process.

2. Material and methods

2.1. Material

The composite system Al-Al₄C₃ has been prepared by powder metallurgy. The starting powders Al (of

size <100 μm) and C (2 wt%) were dry mechanically alloyed for 90 minutes, compacted under the pressure of 600 MPa (rod diameter 40 mm), annealed at 550 °C/3 h and then extruded with 94% diameter reduction; the resulting volume fraction of Al-Al₄C₃ was $V_V = 8\%$, roughly one third of V_V was comprised in very coarse particles. Thin foils of the thickness $L = (2000 \pm 500)$ Å were prepared by spark cutting followed by electropolishing and did not include coarse particles.

Four thin foils have been examined under various magnification M ranging from 42 500 to 80 000. The centres of circles circumscribed to particle images have been chosen as the reference points and the circle diameters served as estimates of particle mean breadths w (cf. Fig. 1).

Only the particles with reference points within the selected rectangular window W of area A have been considered (cf. Table I). For the application of the polygonal method (see below), Voronoi mosaics generated by the point pattern have been constructed (see Fig. 2): a smaller rectangular window W' not including distorted (unbounded) edge cells was chosen and only the cells not intersecting the exclusion line were considered – cf. the reduction in number of points (cells) in Table II. For details cf. [1].

2.2. Preliminary analysis

The unique aim of the preliminary analysis is to confirm that the chosen samples are representative. Consequently, two basic sample characteristics have been evaluated. The sample volume fraction have been roughly estimated using the formula [13]

$$[V_V] = \frac{-2 \ln(1 - [A_A])}{1 + 3L/\bar{w}},$$

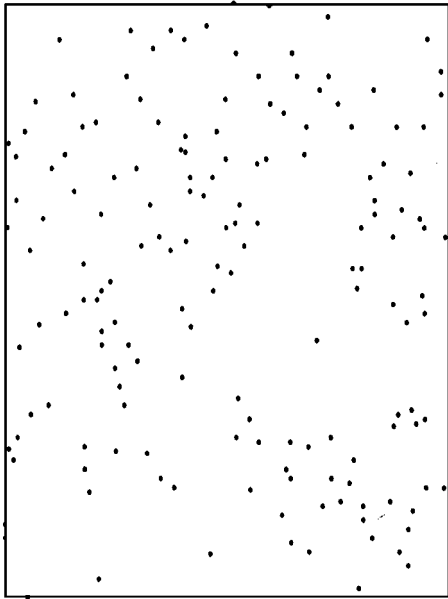


Figure 1 Sample B, the pattern of particle reference points (outlines of particles—see [1]).

TABLE I Results of the preliminary analysis ($L = 2000 \text{ \AA}$)

Sample	M	W (μm^2)	N	\bar{w} (nm)	V_V (%)	λ (μm^{-3})	Δ_{99} (μm^{-3})
A	50 000	7.38	310	72	5.07	154	[131,177]
B	80 000	2.80	200	60	4.80	275	[225,325]
C	80 000	2.78	300	50	3.57	432	[367,496]
D	42 500	9.76	260	76	4.00	96	[81,111]

where $[A_A]$ is the point lattice estimate of the fraction of the projected foil area A covered by particle images and \bar{w} is the average value of the mean breadth w . The formula includes corrections on the particle truncation and overlap of their images. A rough estimate of the reference point intensity (without an overlap correction) is

$$[\lambda] = \frac{N}{A(L + \bar{w})},$$

where N is the number of particles with reference points in the observing window. The results of the preliminary

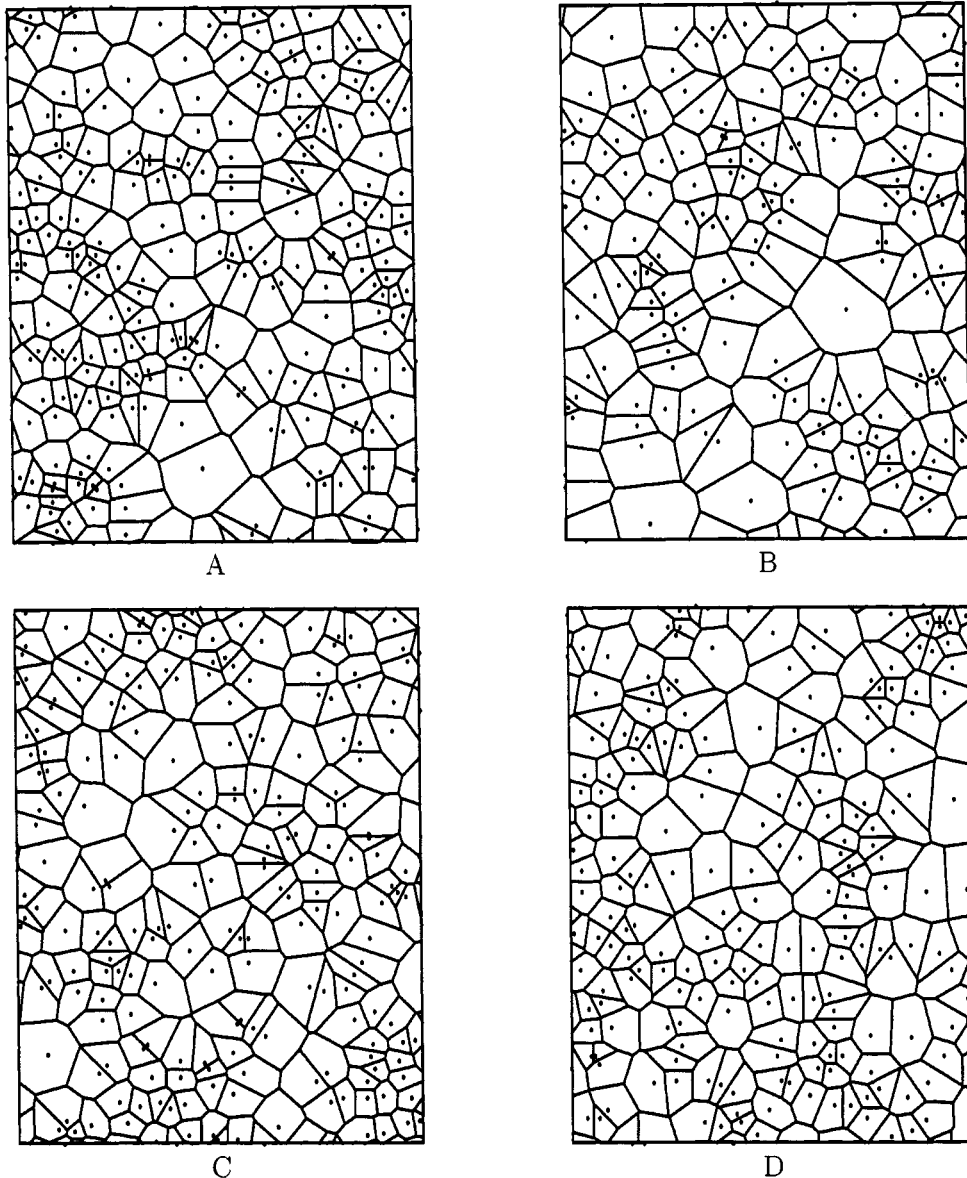


Figure 2 Voronoi mosaics generated by point patterns A, B, C and D.

TABLE II Results of the polygonal analysis ($m_1 = 1$)

Sample	N	m_2	SD (m_2)	m_3	m_4	$\sqrt{b_1}$	b_2	a_0	h (nm)
A	174	0.427	0.123	0.716	2.68	2.585	14.7	0.231	85
B	115	0.644	0.238	1.609	6.72	3.153	16.2	0.184	57
C	150	0.300	0.088	0.361	1.08	2.218	12.0	0.283	57
D	146	0.261	0.045	0.145	0.29	1.098	4.3	0.233	48
PVM	2.10 ⁶	0.281	—	0.154	0.36	1.033	4.6	0.000	—

analysis are summarized in the Table I. The volume fractions in different samples are similar, their values are reasonably close to the expected $V_V = 5\%$ in thin foils. On the other hand, the intensity estimates vary considerably. The deviations can be partly explained by the increase in the resolution power with growing magnification. Nevertheless, the differences between the intensity estimates in samples B, C (observed at the same M) as well as in samples A, D (observed at comparable M) is high enough to indicate an inhomogeneity of dispersion. Assuming that the considered point patterns are samples from a stationary Poisson point process (the subsequent analysis shows that such an assumption is not much unjustified in spite of some important differences), the 99% confidence intervals of the intensity estimates $[\lambda]$, namely $\Delta_{99} = [\lambda](1 \pm u_{0.005}/\sqrt{N})$, have been compared [8, 11] – Table I (here $u_{0.005} = 2.576$ is the 0.005-critical value of the standard normal $N(0, 1)$ distribution. The disjoint confidence intervals confirm the inhomogeneity of samples.

2.3. Estimation of the point pattern arrangement by quadrat count

Quadrat count is a classical method of spatial statistics with many applications [2, 5–8]. The rectangular observing window W is divided subsequently into $m = 2^i$, $i = 2, 3, \dots$ translation equivalent rectangles (quadrats) and the numbers $N_j(m)$, $j = 1, \dots, m$ of points falling into these quadrats are used to estimate the sample mean $N(m)$ and sample variance $s^2(m)$. Under Poisson point process hypothesis, the statistics $ID(m) = (m - 1)s^2(m)/N(m)$ called the *index of dispersion* has the χ^2 -distribution with $m - 1$ degrees of freedom. Two-side 95% confidence interval is usually used for $ID(m)$ and if the null hypothesis is rejected at some values of m with $ID(m)$ being too small, then there is an evidence of regularity (hard-core) in the pattern. Conversely, too great $ID(m)$ reveals a tendency to clustering. Another test statistic $ICS(m) = m^{-1} ID(m) - 1$ called the *index of cluster size* should approach zero under null (Poisson) hypothesis and its distinctly positive (negative) value is an evidence of clustering (regularity) – the expected number $\mathbf{E}n$ of points in clusters would be roughly $ICS + 1$. If a significant departure from the Poisson point process is observed only for certain values of m then the area W/m or the length $\sqrt{W/m}$ can be related to cluster size or regularity scale, respectively (see below).

The results of quadrat count are shown in Fig. 3. Certain tendency to clustering is revealed – especially in the samples A (the highest value of the both indices) and B – at large (small $m \approx 15$) and medium scale (m

between 50 and 100, say). Recalling that the sample size is about 250 points then their mean number is between 2.5 and 5 in the individual medium scale test squares. Taking into account that the value of ICS does not exceed the value of 1, the presence of point pairs only can be expected and their distance must be at least comparable with the mean nearest neighbour distance $0.5/\sqrt{\lambda}$ of the Poisson point process of the same intensity. To confirm this suggestion, several samples of Poisson point process and mild cluster process (Matérn clusters – Poisson distributed number n of points per cluster scattered uniformly at random within a disk of diameter D , see [11]) were simulated with a number of points per square about 200 and compared with the examined samples. Rather similar behaviour of the both indices was observed in the following case: the diameter $D = 1/\lambda$ or $D = 2/\lambda$, the mean number $\mathbf{E}n = 1$; then approximately 60% of non-void clusters are singletons, 30% are pairs and 10% are triads. The both indices behaved rather similarly as the examined specimens at low and medium values of m , see Fig. 3. Obviously no hard-core behaviour was observed at high values of m . The relation between n , D , the interval of m within which a deviation of indices from the Poisson values is observed and the magnitude of this deviation is rather complex. If the size of the elementary quadrat considerably exceeds the size of cluster (its diameter D) then $ICS \approx \mathbf{E}n - 1$ as stated above. Such a situation occurs when m is small but then also the value of ICS considerably oscillates about its mean value depending on the mutual position of the quadrat net and the examined pattern. Even it can happen that no peak at small values of m is observed similarly as in sample C or in one simulated sample in Fig. 3 (note that the presence of clusters can be recognized even when $\mathbf{E}n = 1$).

On the other hand, quadrats small in comparison with D take into account points of a cluster as individual points and no deviation from PPP can be discerned (compare the simulated case $D = 2/\sqrt{\lambda}$ in Fig. 3). Hence it is difficult to decide whether the observed systematic decrease of ICS is due to hard-core features or due to large cluster diameter D .

2.4. Analysis of point patterns by polygonal method

This is a very recent computer based method consisting in the construction of the Voronoi mosaic generated by the examined point pattern [6]. Namely, to any point of the pattern is attached a polygonal (Voronoi) cell formed by all points in the plane of pattern lying closer to this point than to any other point of the pattern. Several characteristics of the mosaic are then measured and

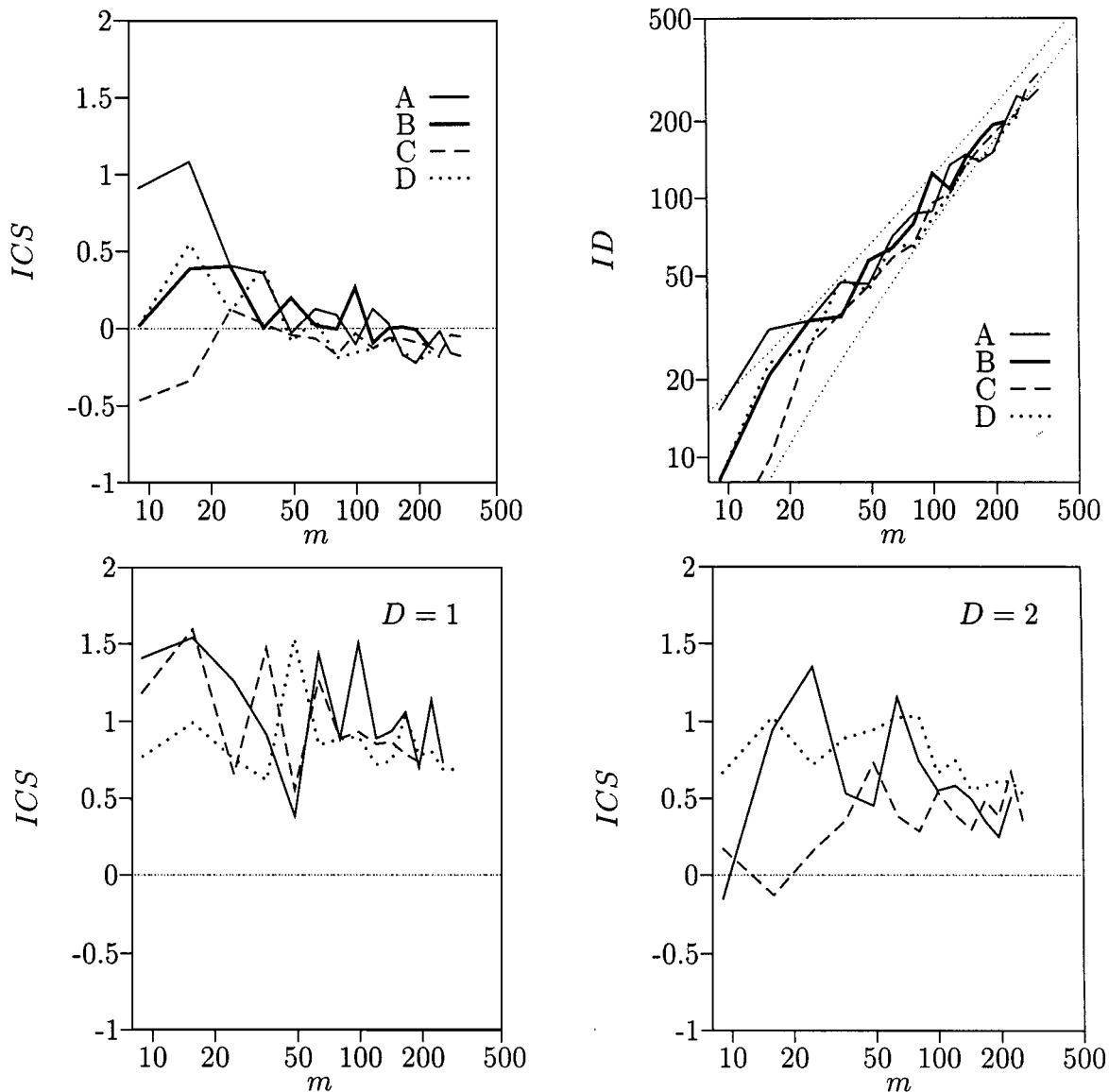


Figure 3 The dependence of indices $ICS(m)$ and $ID(m)$ (with the two-side 95% confidence interval) on the division parameter m for examined specimens and for three simulated realizations of Matérn cluster field with $\mathbf{E}n = 1$ and cluster diameters $D = 1, 2$ ($\lambda = 1$).

compared with the corresponding values of mosaics generated by Poisson point process (Poisson-Voronoi mosaic – PVM) or by other model processes. The size distribution $F_a(x)$ of cell areas a is perhaps the most suitable and arrangement sensitive quantity. The comparison between patterns of various intensity is made by selecting the length unit $[1/\sqrt{\lambda}]$; then the mean value of cell area is $\bar{a} = 1$. The mosaics generated by clustered patterns are overdispersed in comparison with PVM, which means that the moments about origin μ_k as well as related quantities (skewness $\sqrt{\beta_1}$, kurtosis β_2) of area distribution exceeds the corresponding quantities of PVM. The results of polygonal analysis are presented in Table II; N is the number of analysed cells, m_k are the sample moments, $SD(m_2)$ is the standard deviation of the m_2 estimate, $\sqrt{b_1}$ and b_2 are the sample skewness and kurtosis, respectively. a_0 is the nonparametric estimate (c.f. [1]) of the lower bound of $F_a(x)$ distribution, i.e. $F_a(x) = 0$ for $x \leq a_0$. The PVM values obtained by Hinde and Miles [4] are shown for the comparison. It must be stressed that in contrast to the

methods of quadrats where obtained numerical results vary depending on the position of the quadrat net, the Voronoi mosaic generated by the pattern in question is defined unequivocally.

The non-zero values of a_0 indicate that the point pattern has a hard-core character; this is well comprehensible as the original particles do not overlap in space and this feature is not fully lost in the thin foil projections because of low particle intensity and small thickness of the foils ($L/\bar{w} \leq 4$). The rough estimate of the hard-core parameter h (the lower bound of the inter-point spacing) based on a_0 is $[h] = \sqrt{4a_0A/\pi N}$; the obtained values should be lower bounds of the particle breadths w (compare Table I). In view of the poor reliability of estimating bounds of distributions from small samples, the agreement is satisfactory. The value of the hard-core parameter h is well comparable with particle mean breadths and, at the same time, it is as high as the *mean* nearest neighbour distance in a Poisson pattern. Such a pattern differs noticeably from the Poisson point pattern (if it were produced by dependent thinning

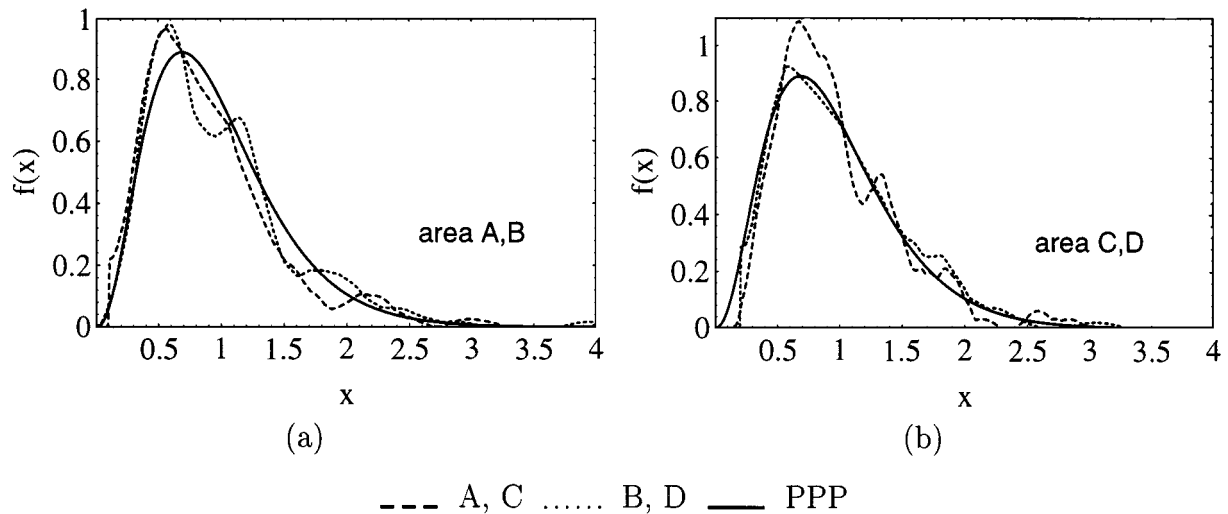


Figure 4 Cell area probability density functions of point patterns A, B, PPP (a) and C, D, PPP (b).

according to the rules of the Matérn hard-core process [11, 12], about 30% of points would be removed) and it can be expected that the values of the moments m_k would be considerably lower than the corresponding values in PVM.

However, any underdispersion with respect to the Poisson point process has not been observed and the sample moments m_k are either comparable with the Poissonian values (samples D, partly C) or considerably higher (A, B). Hence it can be concluded that beside a hard-core arrangement, also clustering at the length scale exceeding h is present in all samples and its degree is high especially in samples A, B. This outcome confirms somewhat less definite results of the quadrat count. In order to prove this hypothesis, the probability density functions (pdfs) $f(x)$ of the cell areas have been estimated using the Epanechnikov kernel estimator [12] ($e_\xi(x) = 0.75(1 - x^2/\xi^2)/\xi$ for $-\xi \leq x \leq \xi$ and 0 otherwise – with the bandwidth $\xi = 0.25$). The results are shown in Fig. 4. For the comparison, also the pdf of PVM is shown (the generalized γ -distribution proposed by Hinde and Miles [4] and based on the large scale simulation was used). The estimated pdf's clearly demonstrate the above proposals: delayed starts of the curves testify hardcores of the points in the patterns whereas shifts of the modes to lower values and slightly heavier (in comparison with PVM) upper tails demonstrate the presence of clustering.

On the other hand, the difference between pdf's is not much pronounced and some quantitative test of their statistical difference is desirable. Consequently, two hypotheses have been proposed, namely

H1: the sets of measured areas are samples (of unequal size) from the same distribution,

H2: the sets of measured areas are samples from the area distribution of PVM,

and the Kolmogorov-Smirnov test was used to examine them (see e.g. [5]). Let $F_{N(Z)}(x)$ be the stepwise empirical distribution function of the cell areas in specimen Z (Z stands for A, B, C, D), where $N(Z)$ is the sample size, and let $F(x)$ be the distribution function of

cell areas in PVM computed by large scale simulations. The test statistics are

$$S1_{Z_i, Z_j} = \sqrt{\frac{N(Z_i)N(Z_j)}{N(Z_i) + N(Z_j)}} D_{Z_i, Z_j},$$

$$i \neq j, \quad \text{and} \quad S2_{Z_i} = \sqrt{N(Z_i)} D_{Z_i},$$

where $D_{Z_i, Z_j} = \max|F_{Z_i}(x) - F_{Z_j}(x)|$ and $D_{Z_i} = \max|F_{Z_i}(x) - F(x)|$. In the framework of the asymptotic approximation, the hypotheses are rejected at the significance level α if $S \bullet_{\{q\}} > k_{1-\alpha}$, where $k_{1-\alpha}$ is the $(1 - \alpha)$ -quantile of the Kolmogorov distribution. In order to avoid the error of the first type (a rejection of a true hypothesis), a small value of $\alpha \leq 0.1$ is usually chosen. However, the reduction of α increases the risk of an error of the second type (a false hypothesis is accepted).

The inspection of the Table III shows, that the both hypotheses can be accepted at the significance levels $\alpha \leq 0.1$, nevertheless **H2** could be rejected for A, B at $\alpha = 0.2$ and at a slightly higher level **H1** could also be false for pairs A, C and B, C. It should be stressed that two deviations from PVM observed in the specimens, namely hard-core features and clustering mutually cancel to certain degree which makes the quantitative analysis more difficult and the results less convincing.

On the basis of observed values of area variances m_2 , a hypothesis concerning number $\mathbf{E}n$ and cluster size can also be proposed. If cluster diameter D is small in comparison with the nearest neighbour distance

TABLE III Results of the Kolmogorov-Smirnov tests

Z_i, Z_j	$S1_{Z_i, Z_j}$	Z_i	$S2_{Z_i}$	$k_{0.8}$	$k_{0.9}$	$k_{0.95}$
A, B	0.763	A	1.166			
A, C	0.999	B	1.200			
A, D	0.764	C	0.763	1.073	1.224	1.358
B, C	1.048	D	0.566			
B, D	0.856	—	—			
C, D	0.535	—	—			

of cluster centres then the variance of the cell areas (generated by Poisson cluster field) is approximately given by $\mathbf{E}n \times m_2(\text{PPP})$ [9]. Hence using the values in Table II, an estimate $1 \leq \mathbf{E}n \leq 2$ follows in agreement with the method of quadrats. A higher value of $\mathbf{E}n$ would be possible if clusters were greater. Also the observed hard-core behaviour can decrease the value of m_2 . The presence of clusters in samples C, D thus cannot be excluded even when the observed $m_2(C)$, $m_2(D) \approx m_2(\text{PPP})$.

The size of clusters can be inferred also from the shape of the pdfs [10] but samples of a greater size would be necessary in order to obtain their more reliable estimates. Other tools of polygonal analysis like order statistics and cell shape analysis are described in [1, 10].

3. Conclusions

It can be concluded, that the both approaches applied to the description of the particle arrangement have given similar results. The polygonal analysis is perhaps more conclusive and its possibilities have not been exhausted in the present treatment. A more detailed comparison of the methods of quadrats and of the polygonal analysis was carried out by Hahn and Lorz [3] for the case of planar sections of 3D Voronoi tessellation. Even if such induced 2D tessellations are not of the Voronoi type, the mutual correspondence between area variances of cell sections and the type of the tessellation generating point pattern is similar, namely higher values of variances describe sections of tessellations generated by cluster fields and any regularity in the pattern is reflected by their decrease. Hahn and Lorz [3] found that independently of the type of the pattern the power of the test based on area variances (sample sizes 100 and 200 points) is definitely higher than that one of the ID test and that the ratio of these powers can be of the order of 2 in more regular structures. Nevertheless, a simultaneous use of the both methods can be recommended if patterns close to PPP are analysed.

It should be stressed, that the main conclusions concerning the spatial arrangement do not require an explicit knowledge of the foil thickness and do not seem to be much influenced by the magnification. Nevertheless, more extensive overlapping of particle images inevitable in thicker foils would make the results less reliable. Recalling the questions posed in the introduction, the results of the analysis are as follows:

ad (1) The samples are representative for the examined composite alloy with respect to included volume fraction of strengthening phase. However, the particle number per unit volume of the foil varies considerably as a function of foil location and used magnification.

ad (2), (3) The Poisson point process is not a suitable model for the point pattern of particle reference points because all examined patterns are combinations of hard-core arrangement with clustering of various degree (increasing in the sequence D, C, A, B) at a coarser scale.

Acknowledgements

This research was supported by the Grant Agency of the Slovak Republic under contract No. 95/5305/483 (M.B., I.K., K.S.) and by the Grant Agency of the Czech Republic under contract No. 201/96/0226 (I.S.).

References

1. M. BESTERCI, I. KOHÚTEK, K. SÜLLEIOVÁ and I. SAXL, *Kovové Materiály* **33** (1995) 251.
2. N. CRESSIE, "Statistics for Spatial Data" (J. Wiley & Sons, New York, 1991).
3. U. HAHN and U. LORZ, *J. Microsc.* **175** (1994) 176.
4. A. L. HINDE and R. E. MILES, *J. Statist. Comput. Simul.* **10** (1980) 205.
5. H. MÜLLER, P. NEUMANN and R. STORM, "Tafeln der Mathematischen Statistik" (VEB Fachbuchverlag, Leipzig, 1973).
6. A. OKABE, B. BOOTS and K. SUGIHARA, "Spatial Tessellations" (J. Wiley & Sons, Chichester, 1992).
7. B. D. RIPLEY, "Spatial statistics" (J. Wiley & Sons, New York, 1981).
8. I. SAXL, K. PELIKÁN, J. RATAJ and M. BESTERCI, "Quantification and Modelling of Heterogeneous Structures (Cambridge Interscience Publishing Company, Cambridge, 1995).
9. I. SAXL and I. KOHÚTEK, in Proceedings of International Conference on the Quantitative Description of Materials Microstructure, Warsaw, edited by L. Wojnar, K. Roźniatowski and K. Kurzydłowski, April 1997, p. 481.
10. I. SAXL, and P. PONÍŽIL, 3D Voronoi tessellations of cluster fields, *Acta Stereol.*, in press.
11. D. STOYAN, W. S. KENDALL and J. MECKE, "Stochastic Geometry and Its Applications" (Akademie Verlag, Berlin, 1987).
12. D. STOYAN and H. STOYAN, "Fraktale, Formen, Punktfelder" (Akademie Verlag, Berlin, 1992).
13. E. E. UNDERWOOD, "Quantitative Stereology" (Addison-Wesley, Reading, MA, 1970).

Received 30 June 1997

and accepted 8 October 1998